

In Press at ApJL

Unravelling Temporal Variability in Saturn’s Spiral Density Waves: Results and Predictions

Matthew S. Tiscareno^{1*}, Philip D. Nicholson¹, Joseph A. Burns^{1,2},
 Matthew M. Hedman¹, Carolyn C. Porco³

¹ Department of Astronomy, Cornell University, Ithaca, NY 14853

² Department of Theoretical and Applied Mechanics, Cornell University, Ithaca, NY 14853

³ CICLOPS, Space Science Institute, 4750 Walnut Street, Boulder, CO 80301

ABSTRACT

We describe a model that accounts for the complex morphology of spiral density waves raised in Saturn’s rings by the co-orbital satellites, Janus and Epimetheus. Our model may be corroborated by future Cassini observations of these time-variable wave patterns.

Subject headings: planets: rings — planets and satellites: individual (Epimetheus, Janus)

1. Introduction

Owing to typical astronomical timescales, a galaxy’s spiral arms are often considered as a fixed pattern. So, too, for the numerous, tightly wound spiral waves detected in Saturn’s rings. In fact, both systems are dynamically active, with waves traveling away from resonant sites. This is manifest only in Saturn’s case, where a pair of moons – Janus and Epimetheus – occupy nearly identical orbits that are interchanged every 4 years, causing the resonance locations in the rings to skip back and forth by tens of km. Since spiral density waves are initiated in Saturn’s rings at locations where ring particle orbits are in a Lindblad resonance with a perturbing moon, the starting points of waves jump as well, allowing wave trains to interfere in complex ways (Porco et al. 2004).

High-resolution images of the rings were obtained by the Cassini spacecraft’s Imaging Science Subsystem (ISS) on 2004 July 1 and on 2005 May 20/21. The calibration and image processing of these data, resulting in a series of brightness scans with orbital radius, along with a catalog of

*Corresponding author: matthewt@astro.cornell.edu

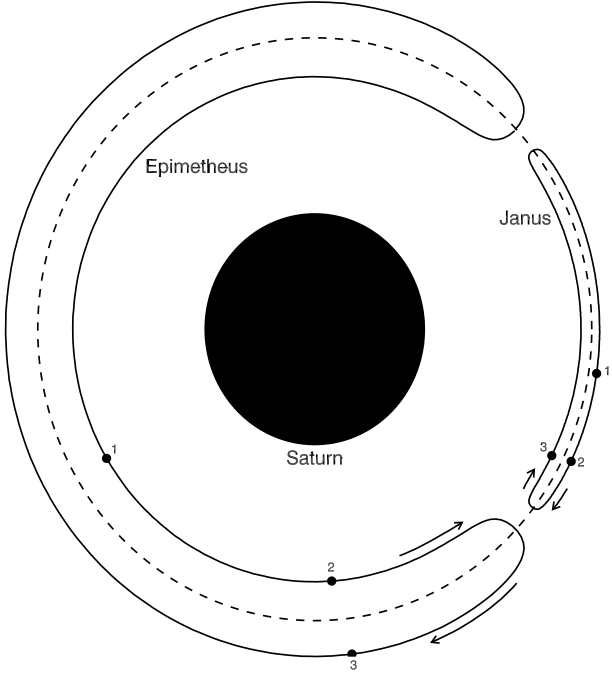


Fig. 1.— The orbits of Janus and Epimetheus (with epicycles removed) in a frame rotating with their mass-averaged mean motion. The radial separation of the librations is exaggerated by a factor of 500. Numbered points mark the moons' positions on 1) 2004 July 1, 2) 2005 May 21, and 3) 2006 September 9. Arrow lengths indicate motion accomplished in 100 days.

important satellite gravitational resonances falling within the rings, are presented by Porco *et al.* (2006, hereafter Paper I). Further analysis of these data, employing techniques derived from the wavelet transform, is presented by Tiscareno *et al.* (2006, hereafter Paper II).

Examination of the Cassini images to date shows that density waves raised by the co-orbitals are both unusual and variable in their morphology. In this paper, we describe a model that accounts for much of the observed structure. We proceed to use this model to predict the future morphology of selected waves at the times and locations of planned Cassini observations, which we expect will test our predictions.

2. The Orbits of Janus and Epimetheus

The orbits of Janus and Epimetheus about Saturn constitute a form of the three-body problem of celestial mechanics that is unique in the solar system (see Dermott & Murray 1981a,b; Yoder *et al.* 1983; Peale 1986). When viewed in a rotating frame of reference, whose angular velocity equals the mass-weighted average of the mean motions of the two moons, Epimetheus executes a

modified “horseshoe orbit” encompassing Janus’ slowly drifting L_3 , L_4 , and L_5 Lagrange points (Fig. 1). However, since Epimetheus’ mass is not negligible compared to Janus’ – the mass ratio is 0.278 (Spitale et al. 2006) – Janus executes its own libration about the average orbit.

Because the orbits of the two moons are so similar ($\Delta a \sim 50$ km), they are commonly known as the “co-orbital satellites” (or, more briefly, the “co-orbitals”). Every 4.00 years, they execute their mutual closest approach and effectively “trade” orbits, the inner moon moving outward and vice versa. The most recent reversal event occurred on 2006 January 21, at which time Janus became the inner satellite and Epimetheus the outer.

3. Spiral Density Waves

Spiral density waves are raised in the rings at locations where ring-particle orbits are in a Lindblad resonance with a perturbing saturnian moon. The density perturbations propagate outward from the resonance location. As reviewed in Paper II (see also Goldreich & Tremaine 1982; Shu 1984; Nicholson et al. 1990; Rosen et al. 1991a,b; Spilker et al. 2004), five parameters characterize the idealized functional form of the perturbation: 1) the background surface density σ_0 , which fixes the wavelength dispersion, 2) the resonance location r_L , specifying a linear translation of the wave, 3) the wave’s initial phase ϕ_0 , 4) the damping parameter ξ_D , indicating a characteristic distance over which the wave propagates before damping away, and 5) the wave’s amplitude A_L , which is proportional to the perturbing moon’s mass.

Considering only co-planar motions, the pattern speed of the resonant perturbation is described by positive integers m and $k+1$; the first giving the number of spiral arms, and the second the order of the resonance (first-order being strongest). A $(k+1)$ th-order Lindblad resonance is generally labeled as $(m+k):(m-1)$.

At a given ring longitude λ , the initial phase of a particular density wave is

$$\phi_0 = m\lambda - (m+k)\lambda_s + k\varpi_s, \quad (1)$$

where λ_s and ϖ_s are the perturbing moon’s mean longitude and longitude of periapse, respectively.

Although previous authors have usually analyzed spiral density waves in Saturn’s rings as static phenomena, in fact they propagate with a finite group velocity (Shu 1984)

$$v_g = \pi G \sigma_0 / \kappa, \quad (2)$$

where κ is the radial (epicyclic) frequency of ring particle orbits, and G is Newton’s gravitational constant. This is the speed at which information (e.g., effects of any change in the resonant forcing) propagates. In the A Ring, v_g is on the order of 10-20 km/yr. Since spiral density waves commonly propagate over many tens of km, and the forcing from the co-orbital satellites changes every 4 yr, discontinuities resulting from reversal events should be observable in density waves raised by the co-orbitals.

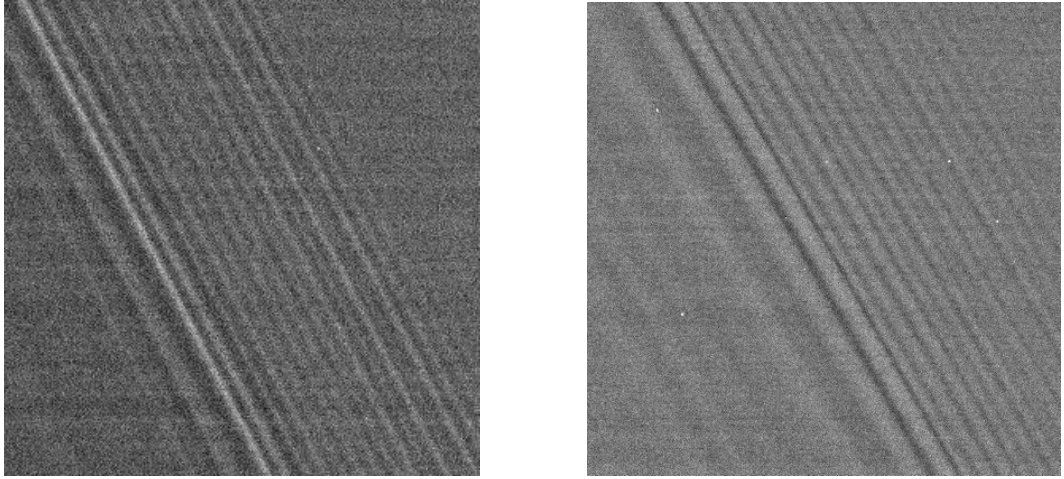


Fig. 2.— Portions of Cassini images a) N1467345385 and b) N1467345916, showing spiral density waves raised by Janus and Epimetheus at the 7:5 and 9:7 resonances, respectively.

4. Data

In the radial scans of ring brightness taken from Cassini ISS images (Paper I), spiral density waves due to the co-orbitals can be discerned at first-order, second-order, and third-order resonances.

First-order waves (e.g., 2:1, 4:3, 5:4, 6:5) were seen by Voyager, and are some of the strongest waves in the ring system. However, non-linear effects, which occur when the density perturbations are comparable to the background surface density, greatly complicate their analysis (Shu et al. 1985; Borderies et al. 1986; Longaretti & Borderies 1986). Not only does the wavelength dispersion deviate significantly from linear theory, but simple superposition of multiple wave segments is not valid.

Second-order waves (e.g., 7:5, 9:7, 11:9, 13:11) were first clearly resolved in the present Cassini data set (Fig. 2). Since the density perturbations comprising these weaker waves are much smaller than the background surface density, they remain well-described by linear theory, and overlapping wave segments can be simply superposed. Accordingly, second-order waves are best-suited for comparison with our simple model, and we will focus exclusively on them.

Additionally, several third-order co-orbital waves can be discerned through wavelet analysis of the radial scans (Paper II); however, these are too weak for much detailed structure to be resolved.

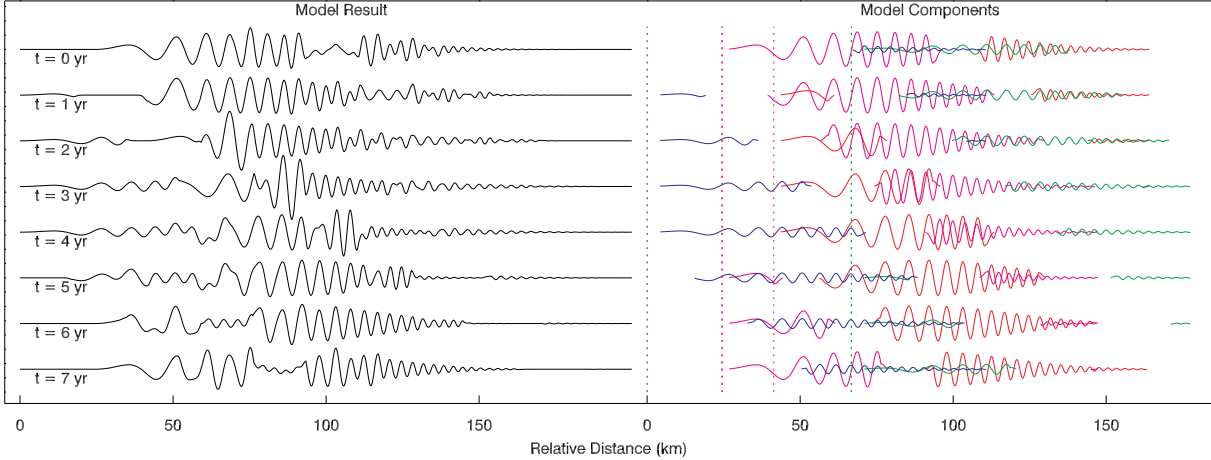


Fig. 3.— An illustration of our model of co-orbital density waves, showing wave morphology at yearly intervals in the 8-yr libration cycle (reversal from JE to EJ occurs at $t = 0$, and from EJ to JE at $t = 4$ yr). Parameters are based on the 9:7 density wave, but here $\phi_0 = 0$ for all wave segments. In the right-hand column are wave segments created by Janus in its inner (purple) and outer (red) configurations, and Epimetheus in its inner (blue) and outer (green) configurations. Only amplitudes larger than 1% are shown. Dotted lines show the resonance locations, with the same color coding. The left-hand column shows the sum of the wave segments, which is the model prediction.

5. Model

Our model is based on a simple assumption: When the co-orbital satellites are in a given configuration (we'll call the Janus-inward configuration JE and the Janus-outward configuration EJ), spiral density waves propagate outward from the current Lindblad resonance locations at the group velocity v_g . When a reversal occurs (e.g., the satellites changing configurations from JE to EJ), the JE resonance locations become inactive; however, the waves previously generated there continue to propagate outwards, resulting in a “headless” wave. Meanwhile, new “tailless” spiral density waves begin to propagate outward at a speed v_g from the EJ Lindblad resonance locations.

At any given time, the locations of “headless” and “tailless” wave segments can be easily calculated from v_g and the elapsed interval since a reversal event. We simply superpose these wave segments atop one another to arrive at a predicted wave morphology (Fig. 3). This time-domain approach to the problem is an alternative to the frequency-domain treatment of Lissauer et al. (1985).

We set the relative amplitude to unity for Janus, and to the moons' mass ratio of 0.278 for Epimetheus. The relevant resonance locations are easily derived from the moons' orbital parameters (Lissauer & Cuzzi 1982, Paper I). The absolute navigation of ISS images is not simple (see

Paper II); nonetheless, all that is necessary for wave morphology is to know the separations among the resonance locations.

The phase of each wave segment (Eq. 1) is determined by what the orbital parameters of the perturbing moon *would have been* had no reversal taken place. This is calculated using high-precision numerically-integrated orbits (Spitale et al. 2006). We make a linear fit to λ_s and to ϖ_s over a single inter-reversal time period, then extrapolate forward to the observation time.

At the end of this process, the only remaining free parameters in our model are the background surface density σ_0 and the damping parameter ξ_D , which respectively control the wavelength dispersion and the propagation distance. We manually adjust these parameters to find the optimum agreement of feature locations between model and data.

For locations at which a wave segment begins or ends, an unrealistically sharp cutoff can occur. We soften such discontinuities by using a half-gaussian, with a characteristic width of 1 km, to bring the perturbation back to zero.

6. Results

Our model results are shown, along with corresponding Cassini image traces, in Fig. 4. We find good qualitative agreement between the two, especially in the “upstream” (left-hand) regions. There is also good agreement between model values of σ_0 and ξ_D and values for nearby waves in the A Ring (9:7, 11:9) and Cassini Division (7:5) (Paper II). We assume that the images are in the normal-contrast regime, given the small optical depth of the regions between opaque self-gravity wakes (Colwell et al. 2006, Paper II)

The most glaring failure of the model occurs in regions where the predicted perturbation is zero (Figs. 4c and 4d). In such regions, the data instead show an oscillatory mode for which we cannot account. It is possible that such oscillations could be raised in the several months during which the resonance locations are migrating from one configuration to the other, which we neglect in treating the reversals as instantaneous events. Another potentially interesting explanation for such oscillations is that a leading spiral density wave may be propagating back towards the resonance location (Shu 1984). This mode is allowed by the mathematical formalism, but has never been observed and has been considered impossible to excite; however, it is conceivable that a “headless” wave could send such a mode into an otherwise undisturbed region.

7. Prediction

Predictions of our model for the times and locations of Cassini ISS observations designed to image the co-orbital waves (Porco et al. 2004) are shown in Fig. 5. Owing to the spacecraft’s low orbital inclination so far this year, the main rings have not been observed at high resolution

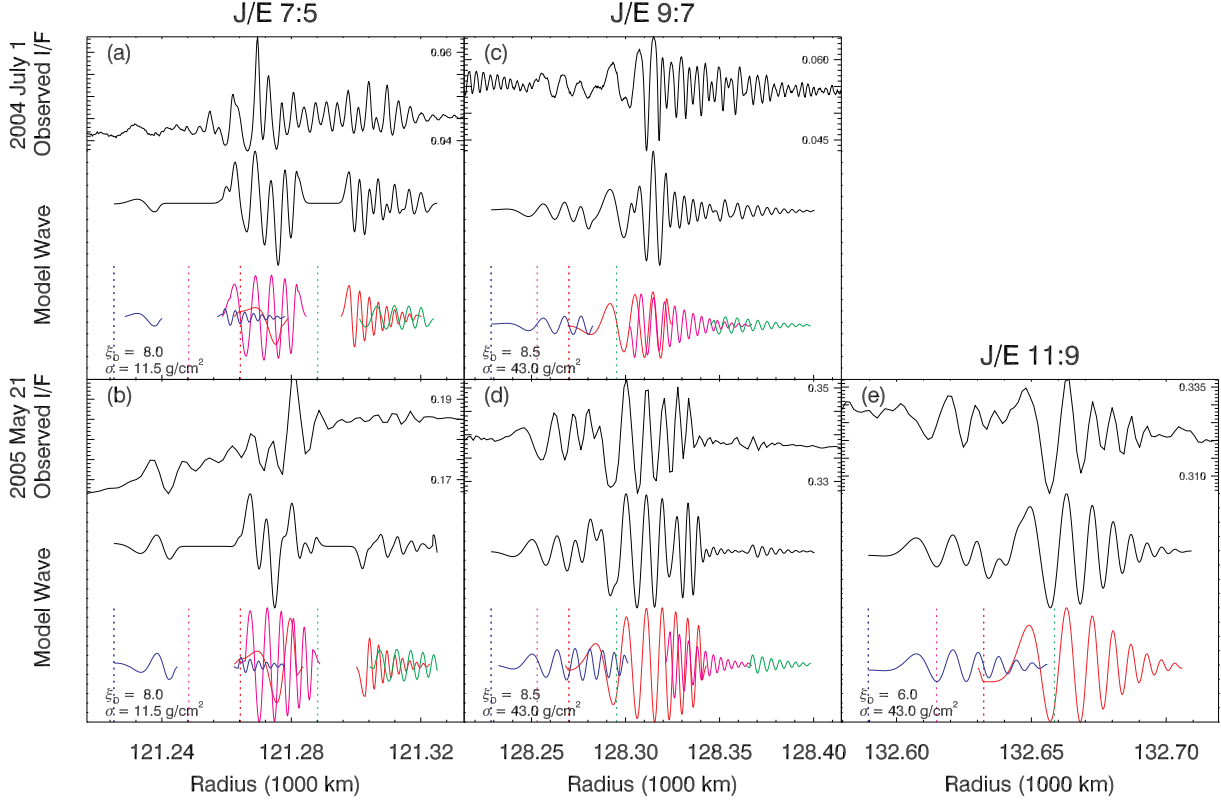


Fig. 4.— Cassini data (Paper I) and model fits for selected Janus/Epimetheus density waves. Resonance label, observation date, surface density σ_0 , and damping parameter ξ_D are given in each figure. Radial traces were taken from the following images: a) N1467345385, b) N1495327885, c) N1467345916, d) N1495326975, e) N1495326431. Image resolutions are 250 m/pixel (a,c) and 1.4 km/pixel (b,d,e). Model resolution has been degraded to correspond to image resolution.

since the last reversal event (from EJ to JE) on 2006 January 21, so the wave patterns in the new configuration have yet to be observed. We predict that the innermost wavecycles (due to Epimetheus in the EJ configuration) will become headless and shift outwards, while a blank gap (possibly containing oscillations as in Figs. 4c and 4d) will appear between the new inner Janus perturbation and the headless perturbation from the outer resonance location.

The next reversal event, expected on 2010 January 21, will be observable only if the Cassini mission is extended beyond the current plan.

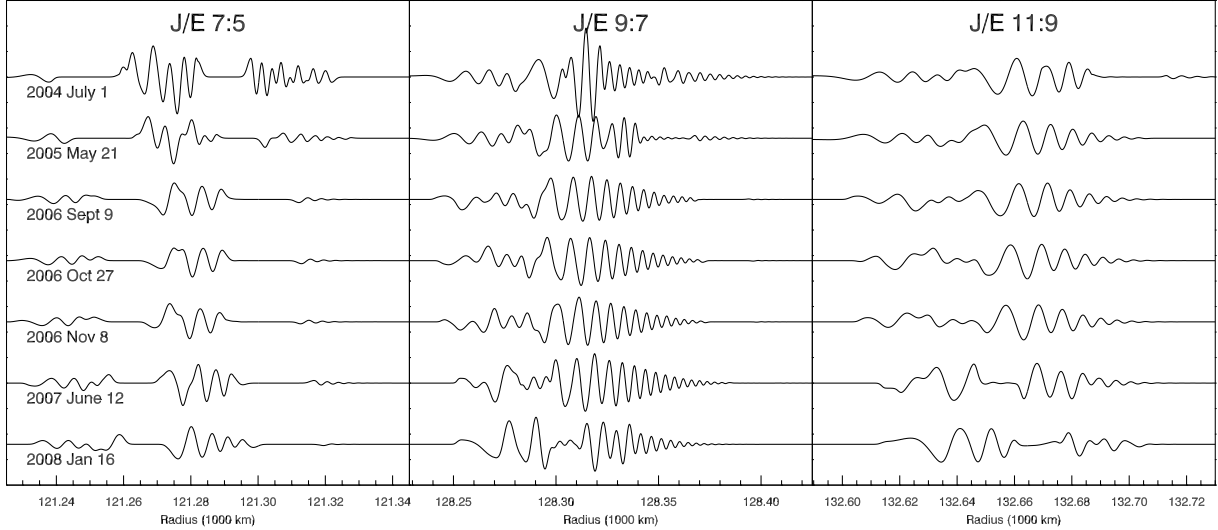


Fig. 5.— Predicted morphology of Janus/Epimetheus density waves at times and locations of past and future Cassini ISS observations. Anticipated image resolutions are 700 m/pixel (2007 June 12) and 1.4 km/pixel (all others).

8. Conclusions

Saturn's rings are a nearby and accessible natural laboratory (Burns & Cuzzi 2006), in which we can observe phenomena of broader interest, such as how a disk responds to variable forcing. Our model is a first step towards a new understanding of the observed complex and time-variable waveforms. We will revisit this topic in more detail, after the accuracy of our predictions (at least for data that will be obtained this year) becomes apparent.

We thank R. A. Jacobson for providing the numerically-integrated satellite orbits. We thank an anonymous reviewer for helping improve the manuscript. We thank those involved in planning and executing the Cassini images, both at JPL and at CICLOPS. We acknowledge funding by Cassini and by NASA PG&G.

REFERENCES

Borderies, N., Goldreich, P., & Tremaine, S. 1986, *Icarus*, 68, 522
 Burns, J. A. & Cuzzi, J. N. 2006, *Science*, 312, 1753
 Colwell, J. E., Esposito, L. W., & Sremčević, M. 2006, *Geophys. Res. Lett.*, 33, L07201
 Dermott, S. F. & Murray, C. D. 1981a, *Icarus*, 48, 1

—. 1981b, *Icarus*, 48, 12

Goldreich, P. & Tremaine, S. 1982, *ARA&A*, 20, 249

Lissauer, J. J. & Cuzzi, J. N. 1982, *AJ*, 87, 1051

Lissauer, J. J., Goldreich, P., & Tremaine, S. 1985, *Icarus*, 64, 425

Longaretti, P.-Y. & Borderies, N. 1986, *Icarus*, 67, 211

Nicholson, P. D., Cooke, M. L., & Pelton, E. 1990, *AJ*, 100, 1339

Peale, S. J. 1986, in *Satellites*, ed. J. A. Burns & M. S. Matthews (Tucson: Univ. Arizona Press), 159–223

Porco, C. C., West, R. A., Squyres, S., McEwen, A., Thomas, P., Murray, C. D., Delgenio, A., Ingersoll, A. P., Johnson, T. V., Neukum, G., Veverka, J., Dones, L., Brahic, A., Burns, J. A., Haemmerle, V., Knowles, B., Dawson, D., Roatsch, T., Beurle, K., & Owen, W. 2004, *Space Sci. Rev.*, 115, 363

Porco *et al.*, C. C. 2006, in preparation (Paper I)

Rosen, P. A., Tyler, G. L., & Marouf, E. A. 1991a, *Icarus*, 93, 3

Rosen, P. A., Tyler, G. L., Marouf, E. A., & Lissauer, J. J. 1991b, *Icarus*, 93, 25

Shu, F. H. 1984, in *Planetary Rings*, ed. R. Greenberg & A. Brahic (Tucson: Univ. Arizona Press), 513–561

Shu, F. H., Dones, L., Lissauer, J. J., Yuan, C., & Cuzzi, J. N. 1985, *ApJ*, 299, 542

Spilker, L. J., Pilorz, S., Lane, A. L., Nelson, R. M., Pollard, B., & Russell, C. T. 2004, *Icarus*, 171, 372

Spitale, J. N., Jacobson, R. A., Porco, C. C., & Owen, W. M. 2006, *AJ*, submitted

Tiscareno, M. S., Burns, J. A., Nicholson, P. D., Hedman, M. M., & Porco, C. C. 2006, *Icarus*, submitted (Paper II)

Yoder, C. F., Colombo, G., Synnott, S. P., & Yoder, K. A. 1983, *Icarus*, 53, 431